Journal of Alloys and Compounds 509 (2011) 7891–7894

Contents lists available at ScienceDirect

Journal of Alloys and Compounds

journal homepage: www.elsevier.com/locate/jallcom

Part II. Large scale applications of $Ni_xMn_{0.8-x}Mg_{0.2}Fe_2O_4$; $0.1 \leq x \leq 0.35$ using laser irradiation

M.A. Ahmed [a,*], Samiha T. Bishay [b], S.I. El-dek [a], G. Omar [a]

[a] Materials Science. Lab (1), Physics Department, Faculty of Science, Cairo University, Giza, Egypt
[b] Department of Physics, Faculty of Girls for Art, Science and Education, Ain Shams University, Cairo, Egypt

ARTICLE INFO

Article history:
Received 29 June 2010
Received in revised form 30 April 2011
Accepted 3 May 2011
Available online 10 May 2011

Keywords:
Ni ferrite
Electrical properties
Laser irradiation

ABSTRACT

$Ni_xMn_{0.8-x}Mg_{0.2}Fe_2O_4$; $0.1 \leq x \leq 0.35$ was prepared by standard ceramic technique at sintering temperature 1200 °C using heating / cooling rate 4 °C/min. The samples were irradiated by Nd YAG pulsed laser with energy of the pulse 250 mJ. X-ray diffractograms reveal cubic spinel structure for all the samples before and after laser irradiation. After laser irradiation, better crystallinity was obtained in a form of an increase in the calculated crystal size. This increase was discussed as due to the change in the valence of some ions like Fe^{3+}, Ni^{2+} and Mn^{2+}. The conductivity of all the investigated samples decreases after laser irradiation and becomes temperature independent for a wider range than that before irradiation. This was ascribed to electron rearrangement after laser irradiation. Accordingly, these ferrites are recommended to be useful in electronic devices.

1. Introduction

The fundamental interaction mechanisms of pulsed laser with solids have greatly stimulated the development of new processing techniques. Key parameters are that the UV laser pulse has an extremely short duration, thus irradiation promotes processes that generally are significantly far from equilibrium. Subsequently, the effect of laser irradiation on the near surface of several ceramic materials of technological relevance will be described [1]. It will be shown through a series of practical examples how a thorough knowledge of these process can be used for manipulating the processing variables to get the desired effect.

The structure and the electrical conductivity of ferrites are very sensitive to the chemical composition [1–6]. Tawfik et al., investigate the effect of laser irradiated on $Co_{0.6}Zn_{0.4}Fe_2O_4$ [7] and reported that a distorted spinel cubic structure was formed after laser irradiation. The conduction was p-type like materials before and after irradiation. The decrease of the electrical resistivity after irradiation was discussed on the basis of the transfer of charge carriers through cation vacancies present at octahedral sites [7]. Singh et al. [8] explained the decrease in dielectric constant and the increase in the dielectric loss parameter for the irradiated $Mg_{0.9}Mn_{0.1}In_xFe_{2-x}O_4$ samples on the basis of Maxwell–Wagner interfacial polarization. Additionally, Ahmed and Bishay [9] found that laser irradiation increase the polarization, resistivity and the paramagnetic region for $Li_{0.5+z}Co_zDy_xFe_{2.5-2z-x}O_4$, $0.0 \leq x \leq 0.2$, $z = 0.1$. They ascribed this behavior to the electron rearrangement after laser irradiations, which create small polaron defects.

The main target of this research work is the creation of new substance with special dielectric behavior useful in several applications. The multivalent ferrite $Ni_xMn_{0.8-x}Mg_{0.2}Fe_2O_4$; $0 \leq x \leq 0.35$ is prepared by standard ceramic technique and a comparative study between the obtained results before and after laser irradiation was an important way to achieve our goal.

2. Experimental

High-purity oxides MnO, NiO, MgO and Fe_2O_3, were mixed in thoroughly stoichiometric ratio, and well grounded in a planetary agate mortar for 3 h. The mixture was pressed into pellets form using uniaxial pressure of 1.9×10^8 Nm^{-2} and pre sintered in air at 900 °C for 10 h with heating rate of 4 °C/min in the Lenton furnace 16/5 UAF (England) then slow cooled to room temperature with the same rate as that of heating. The samples were grounded again for 1 h and pressed into pellets, then finally sintered in air at 1200 °C for 7 h with the same above conditions. X-ray diffraction of these samples was carried out using Philips Pu 1390 channel control Co-kα target and filter Fe of wavelength ($\lambda = 1.791$ Å to assure the formation of the samples with a single spinel phase. Accurate measurements of the electrical resistivity of the samples were carried out on a disc form of ≈0.85 cm diameter and 0.2 cm thickness. The two surfaces of each sample were good polished, coated with silver paste and checked for good conduction. The ac. resistivity as well as the dielectric constant of the investigated samples was carried out from room temperature up to 750 K as a function of frequency ranging from 100 kHz to 5 MHz using RLC Bridge (HIOKI) model 3531 Z Hi Tester "Japan". The measurements were carried out using a home built Lab-View program that is suitable for dielectric measurements. The measuring accuracy was better than 1%. The samples were irradiated to Nd:YAG pulsed laser with energy of the pulse 250 mJ, pulse width 10 ns and beam width

* Corresponding author. Tel.: +202 35676742; fax: +202 35676742.
E-mail addresses: moala1947@yahoo.com, moala47@hotmail.com (M.A. Ahmed).

0925-8388/$ – see front matter © 2011 Elsevier B.V. All rights reserved.
doi:10.1016/j.jallcom.2011.05.007

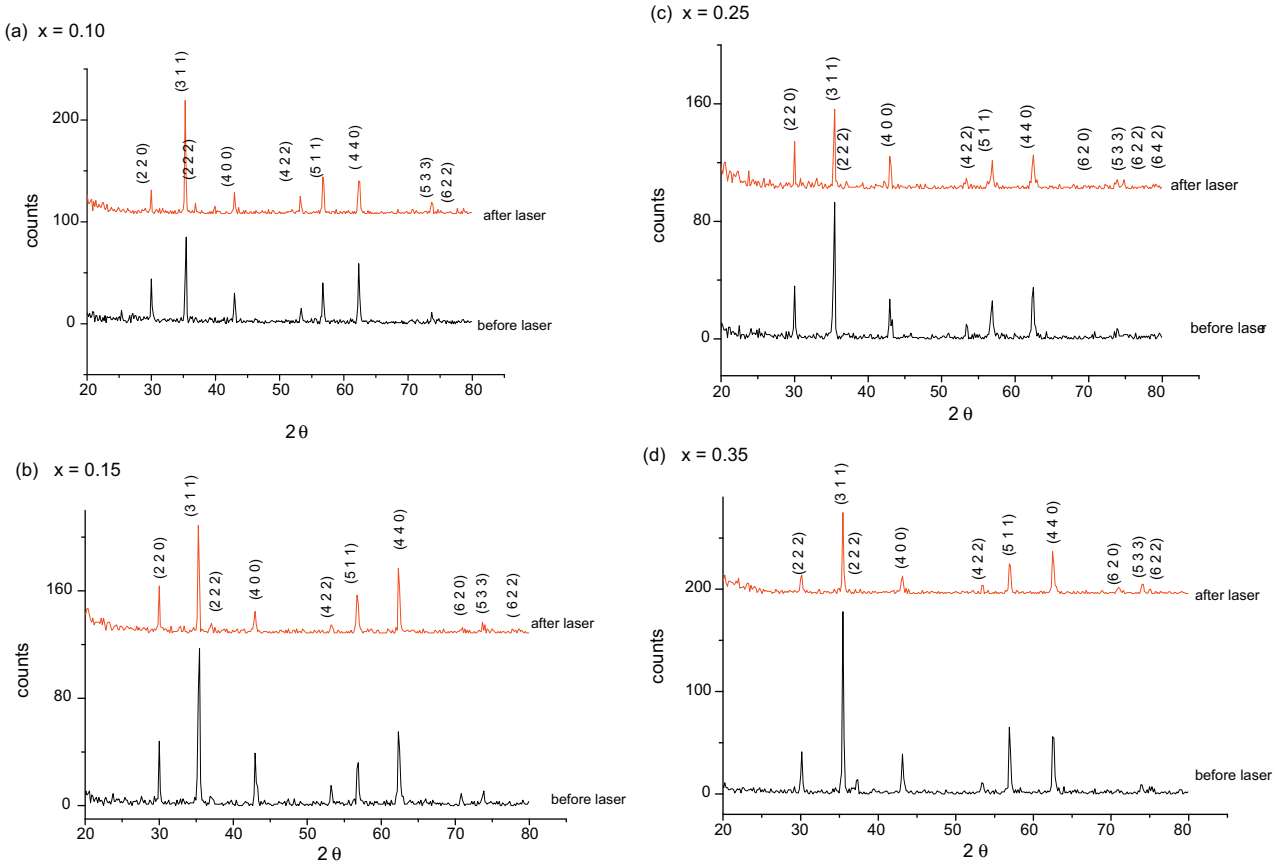

Fig. 1. (a–d) X-ray diffractograms of $Ni_xMn_{0.8-x}Mg_{0.2}Fe_2O_4$; $0 \le x \le 0.35$ before and after laser irradiation.

6 nm. The X-ray analyses and the dielectric measurements were carried out before and after laser irradiation.

3. Result and discussion

Fig. 1a–d shows the X-ray diffraction patterns for the samples $Ni_xMn_{0.8-x}Mg_{0.2}Fe_2O_4$; $0.1 \le x \le 0.35$ before and after laser irradiation. The data shows that X-ray diffractograms of all samples before and after laser irradiation are characteristic of cubic spinel structure as compared and indexed with JCPDS card number 2-1034. All planes identifying the spinel structure appeared (2 2 0), (3 1 1), (2 2 2), (4 0 0), (4 2 2), (5 1 1), (4 4 0), (6 2 0), (5 3 3), (6 2 2). It is noted that for the sample of $x = 0.10$, the crystallinity is improved as it is clear from the intensity of some planes. On the other hand, for the rest of the samples, a disturbance in the cation order, i.e. statistical redistribution of metal cations among A and B sites may be reliable and is accompanied by enhancing of the crystallinity. This was appeared as an increase in the relative intensity of some planes and a decrease in that of another one. The data in Fig. 2 assure that the crystallite size was increased after laser irradiation which agrees well with our mentioned interpretation and those reported by Singh et al. [8].

The average crystal size (L) was calculated from the full width at half maximum (FWHM) of each peak using Debye Sherrer formula [10] as shown in Fig. 2. Before laser irradiation, Ni^{2+} ions occupied the octahedral sites while most of the Mn^{2+} reside on the A site due to site preference and crystal field stabilization energies of both ions. After laser irradiation, valence exchange between similar ions on the same equivalent lattice positions was expected to take place as it is associated by cation redistribution altering the oxygen parameter. Consequently, the crystal size increases.

The percentage porosity (P) was calculated using the relation [11]:

$$P = \left(1 - \frac{D}{D_x}\right) \quad (1)$$

where, D and D_x are the experimental and the X-ray density respectively. The variation of the porosity as a function of Ni content is illustrated in Fig. 3 for the samples $Ni_xMn_{0.8-x}Mg_{0.2}Fe_2O_4$; $0.1 \le x \le 0.35$ before and after laser irradiation. It was found that the porosity has the same trend in the two cases, but with different magnitudes. The value of porosity increases after laser irradiation due to the formation of point and cluster defects, which may exist with the formation of micro cracks.

Fig. 4a and b illustrates the relation between the real part of the dielectric constant ε' and absolute temperature for the sample $Ni_xMn_{0.8-x}Mg_{0.2}Fe_2O_4$; $x = 0.15$ before and after laser irradiation as

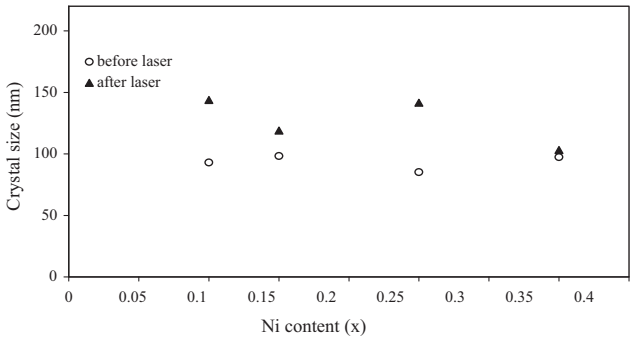

Fig. 2. The dependence of the crystal size on Ni content for the samples $Ni_xMn_{0.8-x}Mg_{0.2}Fe_2O_4$; $0 \le x \le 0.35$ before and after laser irradiation.

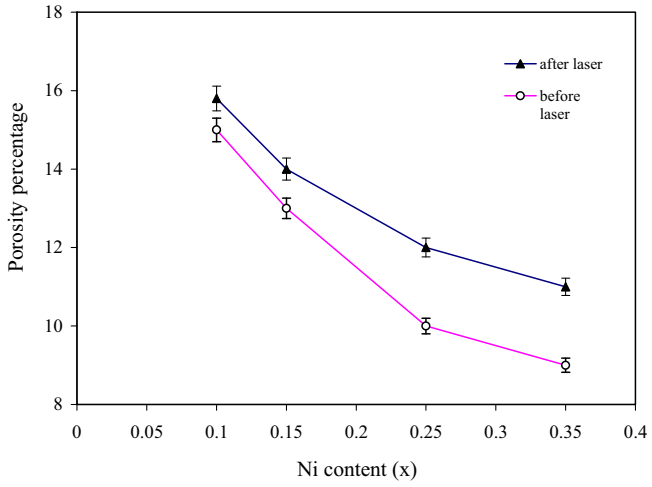

Fig. 3. The dependence of percentage porosity on the Ni content of the samples $Ni_xMn_{0.8-x}Mg_{0.2}Fe_2O_4$; $0.1 \le x \le 0.35$ before and after laser irradiation.

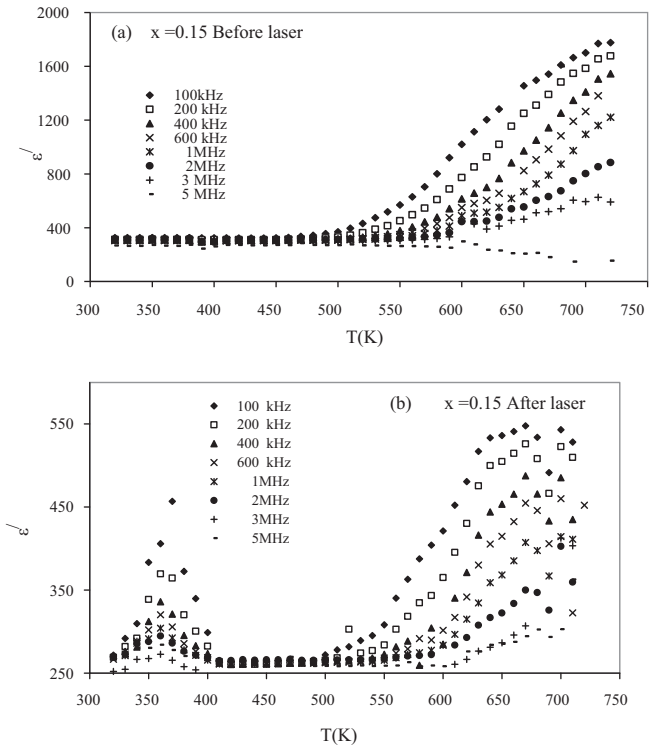

Fig. 4. (a, b) The dependence of the real part of dielectric constant (ε') on the absolute temperature T(K) before and after laser irradiation for the sample $Ni_xMn_{0.8-x}Mg_{0.2}Fe_2O_4$; $x = 0.15$.

a typical curve. In the first temperature region $300 \le T \le 400$, it is clear that a small peak appeared after laser irradiation due to the formation of vacancy cluster pairs [12]. This was enhanced by the increase in the values of porosity as discussed above. From another point of view, after laser irradiation the electronic excitation leads to electronic rearrangements causing some ions and atoms to be displaced from their original crystal positions [9]. Laser induced lattice defects competing with the thermal lattice defects tend to give this small peak.

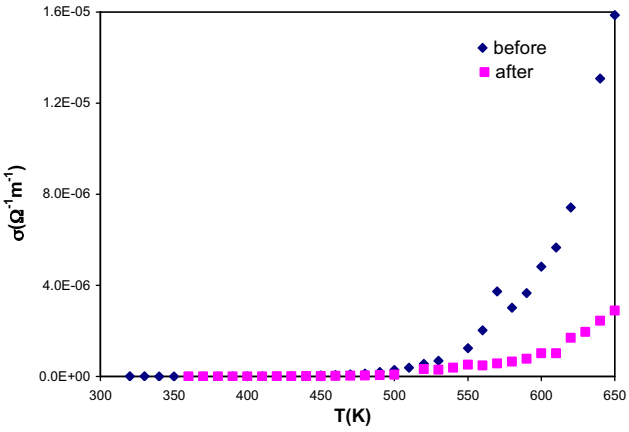

Fig. 5. The dependence of the ac conductivity on absolute temperature at 100 kHz before and after laser irradiation for the sample $Ni_xMn_{0.8-x}Mg_{0.2}Fe_2O_4$; $x = 0.25$.

The dependence of the ac conductivity on frequency is governed by [13]

$$\sigma_{ac} = A\omega^s \quad (2)$$

A is a temperature dependent constant, $\omega = 2\pi f$, f is the frequency and s is the frequency exponent. The values of the exponent (s) are calculated from the slope of the straight line and reported in Table 1 for the samples $Ni_xMn_{0.8x}Mg_{0.2}Fe_2O_4$; $x = 0.1$, 0.15, 0.25 and 0.35 before and after laser irradiation. It is noted that for all the samples (s) decreases by increasing temperature which means that the main conduction mechanism is the correlated barrier hopping and it is the same mechanism before laser irradiation.

For all irradiated samples the variation of σ versus T gave nearly the same trend as that for the samples before irradiation as shown in Fig. 5 as a typical curve for $Ni_xMn_{0.8-x}Mg_{0.2}Fe_2O_4$; $x = 0.25$ at $f = 100$ kHz. The conductivity of the irradiated samples becomes nearly temperature independent for a wide range which is a good applicable result. The irradiation by laser shock waves is followed by the formation of point defects and some of vacancies could react with donor impurities. The conductivity decreases after laser irradiation as a result of higher population of carriers with increasing temperature. This in turns impedes the hopping mechanism by decreasing the drift mobility of charge carriers as a consequence of electron lattice scattering.

The activation energy was calculated using Arrhenius relation from the slope of the line between ln σ and the reciprocal of absolute temperature. Fig. 6 clarifies the dependence of the activation energy in the two regions of temperature E_I and E_{II} on the Ni content for the samples $Ni_xMn_{0.8-x}Mg_{0.2}Fe_2O_4$; $0.1 \le x \le 0.35$ at 100 kHz before and after laser irradiation. It is evident that E_{II} is greater than E_I which is a similar trend before laser irradiation. This means that, in the high temperature region, a large energy is needed to liberate the trapped electrons and activate them to participate in

Table 1
The calculated values of the frequency exponent factor (s) for the samples $Ni_xMn_{0.8-x}Mg_{0.2}Fe_2O_4$ with ($0 \le x \le 0.35$) at selected temperatures before and after laser irradiation.

T(K)	$x = 0.1$		$x = 0.15$		$x = 0.25$		$x = 0.35$	
	Before	After	Before	After	Before	After	Before	After
400	0.73	0.97	0.90	0.62	0.86	0.97	0.90	0.9
600	0.66	0.12	0.25	0.21	0.16	0.08	0.13	0.12
700	0.12	0.11	0.23	0.02	0.12	–	–	–

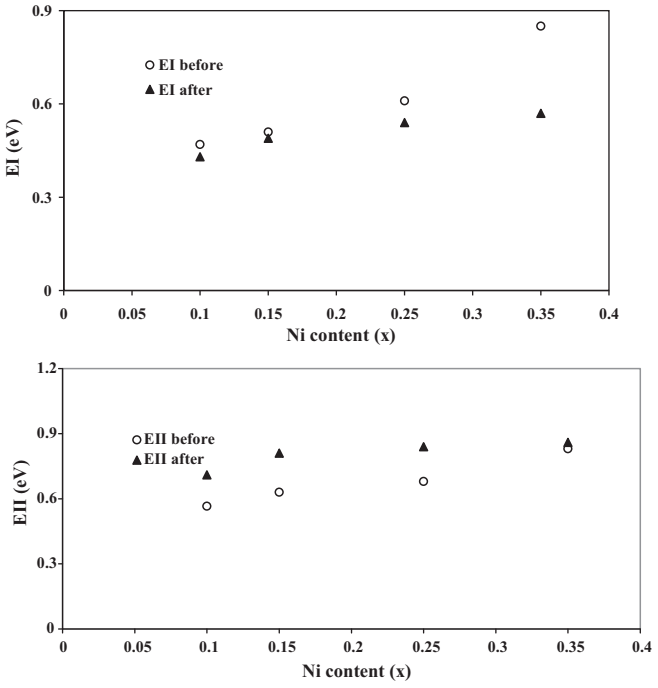

Fig. 6. The dependence of the activation energy E_I and E_{II} (eV) on Ni content for the samples $Ni_xMn_{0.8-x}Mg_{0.2}Fe_2O_4$; $0.1 \leq x \leq 0.35$ at frequency 100 kHz before and after laser irradiation.

conduction process. Also, the figure shows that the calculated values for each one of E_I for all investigated samples decreases after laser irradiation with respect to their corresponding values before irradiation. This may be due to creating small polarons or initiating hole from varying the valences of Ni ions and from another point of view it is due to the effect of spin order.

4. Conclusion

X-ray diffractograms reveal cubic spinel structure for all samples before and after laser irradiation. Better crystallization takes place with the increase in the porosity after laser irradiation. The conductivity of the samples decreases after laser irradiation with a higher thermal stability. The calculated values of E_I decrease after laser irradiation as compared with their corresponding ones before irradiation for all investigated samples.

References

[1] A. Mostafa El-Sayed, Accounts of Chemical Research 34 (2001) 257–264.
[2] M.A. Ahmed, Journal of Magnetism and Magnetic Materials 322 (2010) 763–766.
[3] M.A. Ahmed, N. Okasha, S.I. El-Dek, Nanotechnology 19 (2008) 065603.
[4] M.A. Ahmed, N. Okasha, S.F. Mansour, S.I. El-Dek, Journal of Alloys and Compounds 496 (1–2) (2010) 345–350.
[5] M.A. Ahmed, M.M. EL-Sayed, Journal of Magnetism and Magnetic Materials 308 (2007) 40–45.
[6] Guohong Mu, Xifeng Pan, Na Chen, Keke Gan, Mingyuan Gu, Materials Research Bulletin 43 (2008) 1369–1375.
[7] A. Tawfik, I.M. Hamada, O.M. Hemeda, Journal of Magnetism and Magnetic Materials 250 (2002) 77–82.
[8] M. Singh, A. Dogra, R. Kumar, Nuclear Instruments and Methods in Physics Research B 196 (2002) 315–323.
[9] M.A. Ahmed, S.T. Bishay, Radiation Effect and Defects in Solids 160 (9) (2005) 417–424.
[10] S.A.S. Ebrahimi, J. Azadmanjiri, Journal of Non-Crystalline Solids 353 (2007) 802–804.
[11] M. Kaiser, Journal of Alloys and Compounds 468 (2009) 15–21.
[12] M.A. Ahmed, A.A.I. Khalil, S. Solyman, Journal of Materials Science 42 (2007) 4098–4109.
[13] S.R. Elliott, Advances in Physics 36 (1987) 135.